however, the oxidation rate of NAD(P)H decreased with increasing isoflurane concentration. This implies a dose-dependant inhibition of complex I of the electron transport chain by isoflurane.

Conclusion: Isoflurane exhibits a dual effect on mitochondria, leading to depolarization of mitochondria and inhibition of complex I.

Oxidative Phosphorylation

1559-Pos Modeling Mitochondrial Energetics and Ion Dynamics

An-Chi Wei[1], Miguel A. Aon[2], Brian O'Rourke[2], Raimond L. Winslow[1], Sonia Cortassa[3]

[1] *Johns Hopkins University, Institute for Computational Medicine, Baltimore, MD, USA*
[2] *Johns Hopkins University, Baltimore, MD, USA*
[3] *Johns Hopkins University. Institute for Computational Medicine, Baltimore, MD, USA.*

Board B535

During ischemia, the intracellular environment becomes more acidic and Na^+ loading occurs, affecting not only EC coupling but also the energy supplying machinery. Because ion transport determines mitochondrial pH, volume, and oxidative phosphorylation, we extended a previous single mitochondrion model to account for the dynamics of Na^+, H^+ and phosphate exchange in addition to Ca^{2+} transport, TCA cycle flux and oxidative phosphorylation. The computational model is described by 13 ordinary differential equations, in which the kinetics of each ion carrier has been studied individually to match its behavior in *in vitro* assays. Na^+ transport through the Na^+H^+ exchanger has been modeled as a six-state compulsory order kinetic mechanism. Phosphate transport occurs through a Pi:OH transporter represented by a random bireactant kinetic scheme. The behavior of the assembled mitochondrial model is analyzed and compared with experiments performed with isolated mitochondria. The level of TCA cycle intermediates and the measured flux through the cycle as reported in the literature are well reproduced by the model under steady state conditions. The range of respiratory fluxes simulated corresponds to the physiological range determined in isolated mitochondria. Under transient conditions induced by pulses of ADP or protonophoric uncouplers, the model simulates a decrease in mitochondrial membrane potential ($\Delta\Theta_m$), pyrimidine nucleotide (NADH) levels and an increase in respiratory rate. Conversely, the addition of substrate elicits reduction of the pyridine nucleotide pool and polarization of the membrane. This more comprehensive computational model of mitochondrial energetics and ion transport will improve our ability to study the dynamic changes in EC coupling and energetics during ischemia-reperfusion or metabolic acidosis in the future.

1560-Pos Mathematical Model Of Mitochondrial Energy Metabolism

Ardo Illaste, Marko Vendelin

Institute of Cybernetics at Tallinn University of Technology, Tallinn, Estonia.

Board B536

We present a model of the energy metabolism of the isolatedmitochondrion. The model is composed of a system of ordinarydifferential equations describing the Krebs cycle, oxidativephosphorylation and membrane transport processes. Enzyme catalyzedreactions of the Krebs cycle and some carrier proteins in the model aredescribed by expressions corresponding to their kinetic schemes. Thisassures that the specific reactions adhere to physical limitations setby the overall catalytic capacity of the mitochondrial matrix enzymes.For respiratory chain enzymes an approach based on the thermodynamic properties of the reaction and the system has been taken.In addition to enzymatic reactions the model also takes into account the buffering of protons and metal ions in detail.

The resulting system is optimized to fit the data of several experiments performed on isolated mitochondria. Optimization process consists of applying genetic algorithms and gradient descent methods for finding the set of parameters best suited for reproducing experimental results. Model calculations performed with these optimum parameters are able to fit experimental data and, more importantly, are able to reproduce results from experiments not included in the optimization process.

1561-Pos Different Steady State Kinetics Of Regulation Of Mtck-dependent Respiration In Isolated Mitochondria And Permeabilized Cardiac Cells In Situ:Local Restrictions Of Atp And Adp Diffusion At Outer Mitochondrial Membrane And Enhanced Functional Coupling Of Mtck With Ant

Rita Guzun[1], Natalia Timokhina[2], Tuuli Kaambre[2], Peeter Sikk[2], Claire Monge[1], Valdur A. Saks[1]

[1] *J.Fourier University, Grenoble, France*
[2] *National Institute of Chemical Physics and Biophysics, Tallinn, Estonia.*

Board B537

This work was done to understand better the reason of differences of regulation of mitochondrial respiration in vitro and in permeabilized cardiac cells in situ. It is well known that in permeabilized cells apparent Km for exogenous ADP in control of mitochondria respiration is significantly higher (usually 300 – 400 μM) than in isolated mitochondria (10 – 20 μM). We studied the role of mitochondrial outer membrane in cardiomyocytes in situ for functional coupling between mitochondrial creatine kinase (MtCK) and adenine nucleotide translocase (ANT) following up endogenous ADP fluxes and MtCK kinetics in presence of trapping system PEP-PK for free ADP. In isolated heart mitochondria more than 50% of endogenous ADP recycled by MtCK is trapped in medium by PEP-PK system with apparent Kmapp for MgATP about 0.2–0.3 mM. However, in situ in permeabilized cardiomyocytes, endogenous ADP generated in MtCK reaction is inaccessible for ADP trapping system. This gave us a unique opportunity to perform complete kinetic analysis of the coupled MtCK reaction in the cells in situ by

analyzing respiration rates. While in mitochondria in vitro with oxidative phosphorylation without PK-PEP dissociation constants for MgATP from ternary complex MtCK.Cr.MgATP (Ka) and dissociation from binary complex MtCK.MgATP (Kia) were 0.018 ± 0.007 mM and 0.30 ± 0.06 mM, respectively, in the permeabilized cells these constants were 2.04±0.14 mM and 1.94±0.86, correspondingly. Under these conditions both dissociation constants for creatine, Kb and Kib were equal to2,17±0,40 and 2,12±0,21, respectively. These data show the role of outer mitochondrial membrane in the restriction of permeability for ADP and ATP, and increasing functional coupling between MtCK and ANT.

1562-Pos Regulation Of uMtCK - Dependent Respiration In Rat Brain Mitochondria And Synaptosomes

Claire Monge[1], Nathalie Beraud[1], Tatiana Rostovtseva[2], Dan Sackett[3], Marko Vendelin[4], Valdur Saks[1]

[1] *Universty J.Fourier, Grenoble, France*
[2] *Laboratory of Physical and Structural Biology, Bethesda, MD, USA*
[3] *Laboratory of Integrative and Medical Biophysics, Bethesda, MD, USA*
[4] *Institute of Cybernetics, Tallinn, Estonia.*

Board B538

The role and kinetics of ubiquitous mitochondrial creatine kinase (uMtCK) reaction, functionally coupled to oxidative phosphorylation via adenine nucleotide translocase (ANT) was studied in purified preparations of rat brain mitochondria and synaptosomes. In isolated rat brain mitochondria, oxidative phosphorylation accelerated phosphocreatine production by uMtCK. Complete kinetic analysis showed that oxidative phosphorylation specifically altered only dissociation constants for MgATP, by decreasing dissociation from ternary complex CK.Cr.MgATP (Ka) from 0.13 ± 0.02 to 0.018 ± 0.007 mM and dissociation from binary complex CK.MgATP (Kia) from 1.1 ± 0.29 mM to 0.17 ± 0.07 mM. Dissociation constants for creatine were not changed under these conditions. These data show tight functional coupling of uMtCK with ATP-supply from ANT in brain mitochondria, identical to that of sarcomeric sMtCK and ANT in cardiac mitochondria. In both cases apparent decrease of dissociation constants for MgATP reflects effective cycling of ATP and ADP between MtCK and ANT. Further, in permeabilized synaptosomes apparent Km for exogenous ADP was rather high and equal to 110 ± 11 μM, but decreased to 25 ± 1 μM in the presence of 20 mM creatine. For interpretation of this data, interaction between isolated brain mitochondria and tubulin was studied. Tubulin induced formation of mitochondrial population with a very high apparent Km for exogenous ADP (Km_{app} = 9 ± 1 μM for control and 169 ± 52 μM in presence of 1 μM tubulin). It is concluded that in rat brain cells, particularly in synaptosomes, mitochondrial respiration is under significant control of uMtCK reaction coupled to ANT, and this functional coupling is enhanced due to limitation of outer membrane permeability for ADP by tubulin. These results emphasize important role of phosphocreatine-creatine kinase system in energy transfer in brain cells, including synaptosomes.

1563-Pos Fluorescence-based Biochemistry on Intrinsic Cofactors in Human Breast Normal and Cancerous Cells

Qianru Yu, Ronn Walvick, Ahmed A. Heikal

Penn State University, State College, PA, USA.

Board B539

Reduced nicotinamide adenine (phosphate) dinucleotide (NAD(P)H), and flavin adenine dinucleotide (FAD) are key metabolic cofactors in redox reactions and energy metabolic pathways in eukaryotic cells. As a result, there has been an increasing interest in exploiting these molecules as intrinsic probes for biological processes such as apoptosis and health problems associated with mitochondrial anomalies such as cancer. Here, we provide quantitative biochemistry and structural conformation of intrinsic NAD(P)H using ultrafast dynamics imaging in live, intact breast normal and cancerous cells. In addition to the distinct morphology and mitochondrial distribution in cancer cells, two-photon fluorescence lifetime imaging (FLIM) indicates heterogeneity of the fluorescence lifetime (i.e., quantum yield) distribution in normal and cancer cell environments. These FLIM images enable us to convert the fluorescence intensity into concentration imaging of intrinsic NAD(P)H (172 ± 71 μM in cancer cells and 91 ± 44 μM in normal cells). The observed associated anisotropy, at the single-cell level, also provides a direct quantification of the free (~80%) and enzyme-bound (~20%) percentages of native NAD(P)H. These percentages are further compared with solution studies under enzyme (e.g., mMDH and LDH) titrations. These studies demonstrate the feasibility of conducting biochemistry on intrinsic biomolecules in living cells, which would complement conventional biochemical studies on cell lysates.

1564-Pos Fluorescence Dynamics And Concentration Imaging Of Intrinsic Flavin At The Single Cell Level

Andrew T. Lutes, Ahmed A. Heikal

Penn State University, University Park, PA, USA.

Board B540

Flavin adenine dinucleotide (FAD) exists as a metabolic cofactor in cells. Yet, it remains a challenge to quantify the structural conformation and concentration of cellular flavins as an intrinsic probe for the redox state and energy metabolism in living cells. Here we use several modalities of two-photon (2P) fluorescence lifetime (FLIM) and polarization imaging to quantify the concentration and structural conformation of flavins in normal (HTB 125) and breast cancer (HTB 126) cells. 2P-FLIM reveals that cancer cells exhibit significantly faster average fluorescence lifetime (1.33±0.08 ns, n=5) than their non-transformed counterpart (1.56±0.08 ns, n=7), which is corroborated using single-point magic-angle measurements. Using a newly developed image processing algorithm, 2P-FLIM images were used to convert fluorescence to concentration images of natural

flavin in normal (173±84 μM) and cancer (21±10 μM) cells. In addition, steady-state and time-resolved fluorescence polarization anisotropy measurements indicate a restricted environment of flavin. Comparative studies in buffered solution suggest that enzyme-bound FAD (e.g., LipDH) causes an enhancement of the fluorescence lifetime (i.e., quantum yield) compared with the free molecule. Furthermore, these results are compared with NAD(P)H in cells, which yields results that complement our findings. These results provide new insights into the conformational dynamics and concentration of intrinsic flavins in living cells.

1565-Pos 24 H Hypoxia Of Human Coronary Artery Endothelial Cells (HCAEC) Does Not Alter Cell Viability But Impairs Oxidative Phosphorylation Coupling

Amadou KS Camara, David F. Stowe, Laurel K. Dunn, Stephanie K. Gruenloh, Mohammed Aldakkak, Meetha M. Medhora

Medical College of Wisconsin, Milwaukee, WI, USA.

Board B541

Introduction: Endothelial cells are easily injured because of their location at the blood-organ interface. We hypothesized that alteration of electron transport precedes cell injury following hypoxia-reoxygenation (H-R).

Methods: HCAEC (passages 4–10) were grown to confluence and exposed to normoxia (n=9) or 24h hypoxia (<2% O_2; n=5) followed by 4h of reoxygenation. Cell viability was measured using the MTT assay, trypan blue exclusion, cytochrome c redistribution, and caspase 3 activity. Mitochondrial respiration was measured at 37°C using a Clark O_2 electrode in digitonized cells (1×10^6/ml) suspended in mitochondrial buffer. State 2 respiration was initiated with succinate (10 mM), and coupled state 3 and uncoupled state 3 (3uc) respirations were initiated with ADP (500 μM) or the uncoupler CCCP (4 μM), respectively.

Results: There was no difference in MTT, trypan blue exclusion, mitochondrial release of cytochrome c, or caspase 3 activites between the normoxic and hypoxic group. RCR (respiratory control ratio: state 3/state 4) decreased significantly in hypoxic compared to normoxic cells (1.84±0.40* vs. 2.89±0.44) during ADP coupled respiration (*p<0.05 vs. normoxia). In contrast, uncoupled RCR (RCRuc) was not different between the hypoxic and normoxic cells (2.84±0.55 vs. 3.09±0.43). This damage was evidenced by a larger decrease in state 3 than an increase in state 2 respiration.

Conclusion: The MTT and trypan blue results confirmed the absence of cell death, cytochrome c demonstrated intact mitochondria, and caspase 3 suggested that apoptosis had not been initiated by H-R. Preservation of RCRuc by CCCP demonstrates that H-R does not impair mitochondrial electron flow, but blunts complex V phosphorylation, possibly by promoting ADP -independent proton leak into the matrix.

1566-Pos Structure-function Of The γ-ε-c Interface Of The E. Coli FoF1 ATP Synthase

Shin-Kai Lin, Robert Nakamoto

University of Virginia, Charlottesville, VA, USA.

Board B542

The γ-ε-c subunits of the FoF1 ATP synthase make up the rotor assembly which couples proton transport to catalysis of ATP synthesis or hydrolysis. Previous mutagenesis, functional and EPR studies from our laboratory suggest that interactions among the εγthree subunits play important roles in efficient coupling and we hypothesize that there are conformational changes that must occur during rotation. To further investigate the structure and dynamics of the interface, we have used the site-directed spin labeling strategy of EPR spectroscopy to probe conformational dynamics in the γ-ε subunit interface. EPR spectra of isolated ε subunits with spin-labeled single cysteine substitutions from εG33C to εA39C show an alternating pattern of mobility indicating a β-strand secondary structure. When bound to the F1 complex, spectra of spin-labeled εE29C and εL42C show large decreases of peak-to-peak amplitude, which are likely due to tertiary contacts with the γ subunit. The εL42C as well as the εP40C and εI34C mutant subunits bind to the F1 complex with lower affinity and affect ATP hydrolysis activity indicating that this region of the ε subunit and its interactions with the γ subunit are important for the inhibition function of the ε subunit. The FoF1 membrane with εG37C, εA39C, εP40C, and εA44C mutations synthesize ATP with higher activity and coupling efficiency. Interestingly, the spectra of these four spin labeled F1-bound ε subunits demonstrate lower mobility when F1 is reconstituted with the membranous FO sector, suggesting that these four side chains directly interact with subunit c. These results indicate that the effects of the ε subunit on coupling are mediated through interactions with the c subunit, and the modulation of the ATP catalytic mechanism is at least partially through interactions with the γ subunit.

Supported by PHS grant RO1-GM50957.

1567-Pos Molecular Mechanism of Proton Uptake in the D Channel of Cytochrome *c* Oxidase

Rowan M. Henry[1,2], Ching-Hsing Yu[1,2], Tomas Rodinger[1,2], Régis Pomès[1,2]

[1] *University of Toronto, Toronto, ON, Canada*
[2] *The Hospital for Sick Children, Toronto, ON, Canada.*

Board B543

Cytochrome *c* oxidase is a mitochondrial membrane protein involved in the respiratory pathway. Its role is to utilize the energy liberated by the reduction of molecular oxygen to water to pump protons against an electrochemical gradient. The resulting proton-motive force drives the synthesis of ATP from ADP. Although several high-resolution three-dimensional structures of the enzyme

are known, the molecular mechanism of redox-coupled proton movement remains unknown.

The D channel is a hydrated, 24Å-long cavity within cytochrome *c* oxidase that is thought to be the principal pathway for the water-mediated uptake of chemical protons consumed in oxygen reduction, and of pumped protons, which are translocated across the inner mitochondrial membrane. Among the extensive mutagenesis studies previously performed on the D channel, single-point mutations of N139 and N207 are particularly interesting. Several of these mutations induce decoupled phenotypes, whereby the enzyme does not pump protons but maintains its redox activity, while other mutations compromise both proton pumping and oxygen reduction.

To determine how proton uptake is coupled to the pumping and redox reactions of the enzyme, we examine the relay and delivery of protons to the active site of the wildtype and N139 mutant enzymes. Using molecular dynamics simulations, we combine free energy calculations with large-scale sampling techniques to study the structural and thermodynamic basis of proton movement. Results provide a detailed molecular mechanism of proton uptake and suggest a physical explanation for the mutant phenotypes.

1568-Pos Electrostatic Control of Proton Pumping in Cytochrome c Oxidase

Elisa Fadda

The Hospital for Sick Children, Toronto, ON, Canada.

Board B544

As part of the mitochondrial respiratory chain, cytochrome c oxidase utilizes the energy produced by the reduction of O2 to water to fuel vectorial proton transport. The mechanism coupling proton pumping to redox chemistry is unknown. Recent advances have provided evidence that each of the four observable transitions in the complex catalytic cycle consists of a similar sequence of events. However, the physico-chemical basis underlying this recurring sequence has not been identified. We identify this recurring pattern based on a comprehensive model of the catalytic cycle derived from the analysis of oxygen chemistry and available experimental evidence. A sequence of three distinct electrostatic states recurs identically four times per turnover despite differences in the redox chemistry. This model leads to a simple, robust, and reproducible sequence of electron and proton transfer steps and rationalizes the pumping mechanism in terms of electrostatic coupling of proton translocation to redox chemistry. Continuum electrostatic calculations support the proposed mechanism and suggest an electrostatic origin for the decoupled and inactive phenotypes of ionic mutants in the principal proton-uptake pathway.

1569-Pos Electrochemically induced Electron Transfer into Cytochrome c Oxidase (CcO) Monitored by Time Resolved Surface-Enhanced ATR-FTIR-Spectroscopy

Vinzenz U. Kirste[1], Marcel G. Friedrich[2], Renate L. C. Naumann[1], Wolfgang Knoll[1]

[1] *Max Planck Institute for Polymer Research, Mainz, Germany*
[2] *Harvard University, Cambridge, MA, USA.*

Board B545

Cytochrome c Oxidase (CcO) is investigated using time-resolved Surface Enhanced ATR-FTIR Spectroscopy. Electrons are injected into the protein by direct electron transfer from the gold electrode on the silicon crystal of the ATR-IR setup. For this purpose, the CcO is immobilized via his-tag-binding with the cytochrome c binding site directed towards the electrode. The immobilization is followed by an in-situ reconstitution into a bilayer lipid membrane.

Structural changes of the peptide backbone are deduced from spectral changes of certain bands (e.g. Amide I), which are assigned to specific redox states of the redox centers.

These spectral changes are monitored by Surface Enhanced ATR-FTIR Spectroscopy in the rapid scan and in the step scan mode.

Stationary measurements at different fixed potentials show that redox transitions occur in all four redox centers. Time-resolved measurements, applying repeated potential pulses allow to follow the change of the redox state of the Cu-A, the heme a and the heme a3 center as a function of time. Time constants of the transitions are obtained by fitting three parameter exponentials to the time dependent absorption data.

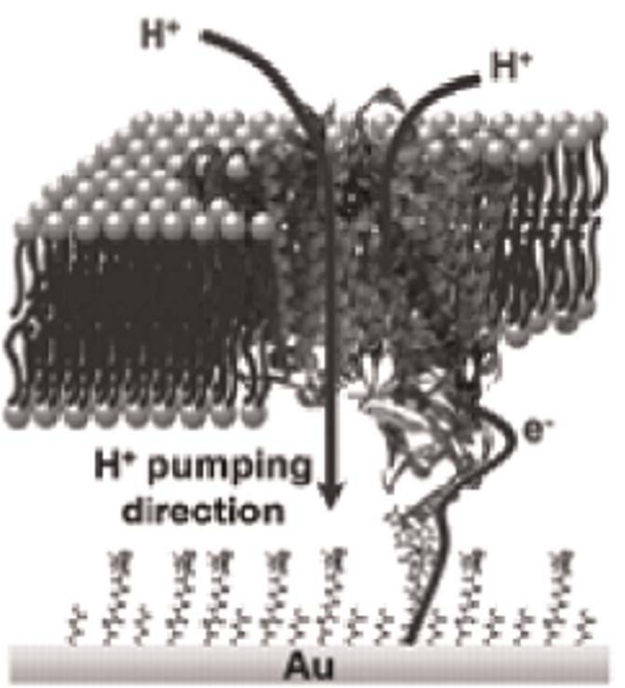

1570-Pos Ethanol Suppresses Respiration Stimulated by Ureagenic Substrates in Cultured Rat Hepatocytes: Partial Reversal by Inhibition of Alcohol Dehydrogenase and Cytochrome P450 but not by Acetaldehyde Dehydrogenase

Christoph Czerny

Medical University of South Carolina, Charleston, SC, USA.

Board B546

BACKGROUND. Ethanol is a hepatotoxicant to humans that alters hepatic metabolism. Ethanol undergoes 2-step oxidation to acetaldyhyde in the cytosol by alcohol dehydrogenase (ADH) and cytochrome P450 2E1 (2E1) and then to acetate by acetaldehyde dehydrogenase (ACDH) in mitochondria. Previous studies showed that ethanol suppressed mitochondrial metabolism in permeabilized hepatocytes (*BBA* **1762**, 181). The goal of this study was to determine the effect of ethanol metabolism on mitochondrial respiration in intact hepatocytes.

METHODS: After 18 h in culture, rat hepatocytes in Krebs-Ringer-HEPES buffer were treated with ethanol (0–100 mM) and ureagenic substrates (in mM: 3 NH_4Cl, 5 L-ornithine, 5 Na-lactate) in the presence and absence of cyanamide (200 μM, 2E1 inhibitor), 4-methylpyrazole (4-MP, 100 μM, ADH inhibitor) or aminobenzotriazole (ABT, 1 mM, ACDH inhibitor). Oxygen consumption rate (OCR) was measured with a Seahorse XF24 analyzer.

RESULTS: Ureagenic substrates doubled OCR with an initial 25% stimulation within 5 min followed by a progressive increase over the next 45 min. Ethanol dose-dependently suppressed OCR stimulated by ureagenesis with half maximal inhibition at ~50 mM. At 100 mM, ethanol suppressed stimulated OCR by >80%. In the presence of 100 mM ethanol, cyanamide and 4-MP restored stimulated OCR by 18 and 26% respectively and in combination restored OCR by 36%. ABT did not prevent suppression of stimulated OCR by ethanol.

CONCLUSIONS: ATP demand created by ureagenesis stimulates respiration by cultured hepatocytes. Ethanol suppresses this stimulation, an effect partially reversed by ADH and 2E1 inhibitors but not by inhibition of ACDH. Thus, ethanol-dependent suppression of mitochondrial respiration may be the consequence, at least in part, of cytosolic generation of acetaldehyde and/or NADH.

X-Ray Diffraction

1571-Pos Hybrid Methods In The Structure Determination Of Extremely Large Proteins

Thomas Barends[1], Kay Büchler[2], Christos Gatsogiannis[3], Ilme Schlichting[1], Jürgen Markl[3], Heinz Decker[2], Elmar Jaenicke[2]

[1] *Max-Planck Institute for Medical Research, Heidelberg, Germany*
[2] *Institut für Molekulare Biophysik, Johannes Gutenberg Universität, Mainz, Germany*
[3] *Institut für Zoologie, Johannes Gutenberg Universität, Mainz, Germany.*

Board B547

Gastropod hemocyanins are extremely large oxygen transport proteins (8MDa), which cooperatively bind oxygen at type-3 copper centers. Native hemocyanin is a cylindrical didecamer made up from a subunit (400kDa), which contains 7 homologous functional units (FU, 50kDa) and one FU (FU-h) with an additional tail of ~100aa. While the structure of two FUs is known, the spatial arrangement of the FUs within the didecamer and the fold of the FU-h tail remain unclear. We use a hybrid method, i.e. 3D-cryo-electron microscopy and X-ray crystallography, to obtain structural information.

The enormous size of hemocyanin makes protein crystallography daunting but not impossible. We grew crystals of a cephalopod hemocyanin (3.5MDa, *Octopus*), which represents one half of a gastropod hemocyanin. These crystals diffracted to a resolution of 4Å at room temperature. Due to their radiation sensitivity cryo conditions were used for data collection, which as a side effect reduced the diffraction limit to 7Å. The dataset shows a small peak in the self-rotation function at ξ=72°, as expected from the fivefold symmetry of hemocyanin. Using this peak to fix the orientation of the five-fold axis, we wish to use molecular replacement with low-resolution models to obtain starting phases for these data.

Conversely, X-ray structures may be placed in the 3D-density map obtained from cryo-EM experiments. FU-h from keyhole limpet hemocyanin was crystallized and a 4Å dataset was collected, which was phased with molecular replacement. The major part of FU-h has the canonical fold of a molluscan hemocyanin FU, but surprisingly the C-terminal tail displays a typical cupredoxin fold. Thus, FU-h combines a type-3 copper protein fold in the N-terminal region with an unexpected type-1 copper protein fold at its C-terminus.

Financed by DFG and BMBF

1572-Pos Physical Properties of Cryoprotective Solutions for Cryo-Crystallography

Thomas Alcorn, Douglas H. Juers

Whitman College, Walla Walla, WA, USA.

Board B548

Macromolecular crystallography has undergone a major transformation in the last decade, in which most structures are now determined at cryogenic temperature in order to minimize crystal degradation from radiation damage effects. The cryogenic cooling process, however, is still accomplished mostly via trial and error. Cooling can induce crystal damage, and minimizing this damage is still somewhat of an art form. One way of minimizing cooling-induced damage is to supplement the crystal storage solution with cryoprotective molecules, called cryoprotectants. Many different cryoprotectants have been used for cryo-crystallography, although glycerol is probably the most common. There are, however, few general principles available to guide researchers in deciding on the makeup of the cryoprotective solution. To help fill this gap, we present the results of our efforts to characterize the physical properties of cryoprotective solutions. We measured the contraction of binary solutions (50 % w/w) of cryoprotectant and water when rapidly cooled from room temperature into